ELSEVIER

Polymer 42 (2001) 7381–7394

polymer

www.elsevier.nl/locate/polymer

Phase morphology, crystallinity and mechanical properties of binary blends of high barrier ethylene–vinyl alcohol copolymer and amorphous polyamide and a polyamide-containing ionomer

J.M. Lagarón[a,*], E. Giménez[a], J.J. Saura[a], R. Gavara[b]

[a]*Department of Technology, Area of Materials, Universitat Jaume I, Campus Riu Sec, Castellon 12071, Spain*
[b]*Instituto de Agroquímica y Tecnología de los Alimentos, CSIC, Apdo. Correos 73, 46100 Burjassot, Spain*

Received 9 November 2000; received in revised form 13 March 2001; accepted 14 March 2001

Abstract

A number of dry melt-mixed binary blends of 32 mol% ethylene vinyl–alcohol copolymer (EVOH) and an amorphous polyamide (PA) and a crystalline Nylon-containing ionomer have been characterized in terms of phase morphology, crystallinity and mechanical properties by DSC, WAXS, DMA, SEM, microhardness (MH) and tensile testing. Such blends are claimed by manufacturers to improve the thermoformability characteristics of EVOH while retaining/improving its high gas barrier under high relative humidity conditions. From the results, it becomes apparent that the miscibility of this high barrier EVOH grade with the amorphous PA is very poor, and clear phase segregation throughout composition was shown by DSC, DMA and SEM. Factors like geometric hindrance and chain stiffness of the amorphous PA could be responsible for this behavior. A lack of good interaction between EVOH/PA blend components was further supported by the negative deviation from the simple additive rule seen in the mechanical properties of these blends. A two phase structure was also observed in the EVOH/ionomer blends, but from the results a better phase compatibility was inferred. This compatibility increased in the ionomer rich blends and was thought to be enhanced by the presence of crystalline Nylon in the formulation of the ionomer. An increased in flexibility and toughness was measured in the mechanical properties of these EVOH/ionomer blends. The flexibility rose with increasing strain rate in extruded films. The overall crystallinity of the blends was lower than that of neat EVOH, ought to the amorphous condition of the PA and the lower crystallinity exhibited by the ionomer.

Keywords: High barrier ethylene vinyl–alcohol copolymers; Blends; Nylon-containing ionomer

1. Introduction

Ethylene–vinyl alcohol copolymers are a family of random semicrystalline materials with excellent barrier properties to gases and hydrocarbons, and with outstanding chemical resistance. These copolymers are therefore being increasingly used in the packaging industry as barrier layers to protect foods from the ingress of oxygen and losses of flavors and consequently to increase package shelf-life [1]. Their barrier properties increase with increasing the content of vinyl alcohol in the grade. Accordingly, compositions of vinyl alcohol higher than 56 mol% are preferred. In particular those grades with higher content of vinyl alcohol ($\geq$68 mol%) have outstanding barrier to gases [1] like O_2, N_2 and CO_2 and to hydrocarbons [2]. EVOH copolymers are highly crystalline materials, albeit their properties are largely dependent on composition. The use of the parent polymer polyvinyl alcohol is not practical because it has a melting point very close to the onset of degradation and it is very sensitive to plasticization by water. Nevertheless, EVOH copolymers are also largely affected by water and possess a number of processing associated problems, like deficient thermoformability, due to high crystallization kinetics [3]. In addition to low moisture resistance, EVOH copolymers do not have a good compatibility (adhesion and miscibility) with other polymers whether of polar or non-polar nature [4]. The lack of good compatibility with other polymers is thought to be a consequence of the fact that EVOH copolymers are strongly self-associated, while the inter-association of the hydroxyl groups of EVOH with, for instance, the carbonyl groups of complementary polymers is comparatively weak. Even miscible systems have low Lower Critical Solution Temperatures (LCST) and phase separation is anticipated at processing temperatures. In order to avoid the deterioration of the physical and barrier

* Corresponding author. Tel: +349-64-728-137; fax: +349-64-728-106.
E-mail address: lagaron@sg.uji.es (J.M. Lagarón).

0032-3861/01/$ - see front matter
PII: S0032-3861(01)00204-X

properties by the uptake of water these materials are usually sandwiched by coextrusion in multilayer structures where an inner and outer layer of an hydrophobic material, e.g. polyethylene, wrap up the barrier layer made up of EVOH. Blends of EVOH with other materials have been profusely studied over the last years with the aim of boosting the barrier properties of low barrier performance materials, improving mechanical properties of EVOH and/or adhesion, etc. [5–9].

Melt-mixed blends of EVOH (32 mol% ethylene) and polyamide 6 (PA6) have been reported [8] to show some miscibility as revealed by melting point depression and positive deviation from the simple additive rule in complex viscosity and tensile properties. Changes during melting and crystallization and in the relaxational behavior of these blends were also observed by Petris et al. [6], although a biphasic nature was revealed by microscopic observations. The difficulty associated with the DMA analysis of EVOH/PA6 blends in terms of miscibility was put forward by Russo et al. [10] due to the closeness of the neat polymer T_g's. In any case, by curve fitting the loss modulus signal these authors proposed a single T_g occurrence for the blends attributable to a single glass-rubber transition. Ahn et al. [12] studied a number of blends of EVOH with PA6, PA6/12 and PA12. These authors found homogeneous phase morphologies in the PA6 rich blends and a fine phase separation in the EVOH rich blends. On the contrary, clean phase separation in large domains were observed in EVOH/PA6/12 and EVOH/PA12 blends. Lower critical solution temperature was identified by Akiba et al. [12] immediately above the melting point of blends of 59 mol% EVOH and PA6/12. Nevertheless, 32 mol% EVOH blends with PA6/12 were found to be immiscible from melting to degradation temperatures. Miscibility in blends of EVOH and PA6/12 was also found to be dependent on the ratio PA6 to PA12 by Uno et al. [9]. Blends of EVOH and PA6/6.9 were found to be partially miscible by Nir et al. [13], albeit EVOH rich blends exhibited much lower miscibility. In all cases compatibility was attributed to interpolymer molecules hydrogen bonding. Blends of amorphous PA with PA6 showed compatibility, but also metastability [14]. Annealing above T_g induced phase separation due to crystallization and differences in polymer stiffness and spatial geometry.

It is well known that the EVOH solid phase formability window, usually between 90 and 110°C, does not overlap with that of many polymers used in coextrusion to form multilayer structures in the packaging industry. For example, the optimal thermoformability window for polypropylene falls between 145 and 160°C and for polystyrene between 110 and 135°C. Blends of EVOH with low contents of amorphous PA are claimed by manufacturers to broaden the forming capacity of EVOH with respect to temperature and draw ratios without sacrifice in gas barrier properties [3]. Amorphous PA exhibits a much better forming capability and its gas barrier performance [15] improves with increasing relative humidity as opposed to EVOH, which barrier properties deteriorate with increasing relative humidity [16,17]. Blends of EVOH with an ionomer, Zn^{2+} (random 78/10/12 ethylene–methacrylic acid–isobutylacrylate terpolymer with a degree of neutralization of ca. 70%) were studied by Samios et al. [5]. The role of the ionomer was envisaged to serve as a good compatibilising agent between EVOH and other polymers like polyethylene. These blends showed phase separation (in particular, in EVOH rich blends), two T_g's approaching each other, slight EVOH melting point depression, reduced crystallinity, increased flexibility and toughness. As a result, a strong association between components was suggested by the authors, possibly due to hydrogen bonding and/or ionic interactions. Nylon containing, partially neutralized, ethylene–methacrylic acid copolymers (ionomer) are a family of materials highly transparent and with low hygroscopicity. These ionomers are thermoplastic materials ionically crosslinked and their properties vary with molecular weight and the amount of crosslinking. These materials are designed to be tumble-blended with EVOH in conventional equipment and are claimed [18] to provided a soft, clear, flexible film or sheet with improved flex resistance, excellent thermoformability, and gas barrier at high humidity, compared to films made of EVOH alone. In this study, a thorough characterization of the blend morphology, crystallinity and mechanical properties of a number of binary blends of EVOH with amorphous PA and crystalline PA-containing ionomer was carried out. The influence of the relative humidity on the blends will be the subject of a further work.

2. Experimental

2.1. Materials

A number of binary blends of commercially available ethylene-vinyl alcohol copolymer (EVOH with 32 mol% of ethylene, EVAL® LCF-101) from Kuraray, amorphous polyamide (Selar® PA UX-2034, polymerized by condensation of hexamethylene diamine and a mixture of 70/30 isophthalic and terephthalic acids) and nylon-containing ionomer (Surlyn® AM-7938) from DuPont de Nemours were prepared by melt mixing at 230°C during 10 min at 30 rpm in a Brabender mixer under an inert atmosphere. The random placement of the acid isomers in the polymer chain prevents crystallization in the amorphous PA. The ionomer is a crystalline nylon containing partially neutralized ethylene methacrylic acid copolymer. The type and content of the crystalline nylon present in the ionomer was not supplied by the manufacturer. Sample sheets were obtained by compression molding in a hot plate press at 220°C followed by quenching in water. Specimens of EVOH/PA blends were dried at 110°C for four hours before testing and EVOH/ionomer blends were dried at 70°C for 48 h in a vacuum oven due to the low melting point exhibited by

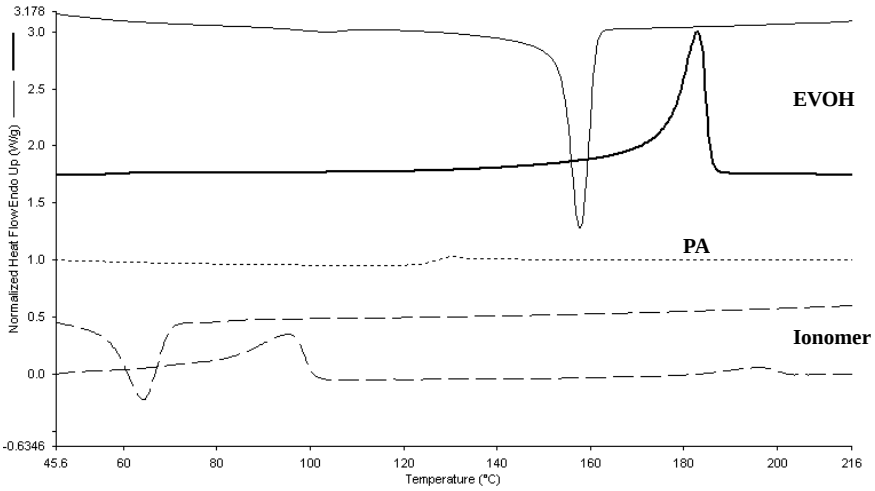

Fig. 1. DSC crystallisation exotherms and melting endotherms of EVOH (continuous curves), amorphous PA (dotted curve) and polyamide-containing ionomer (dashed curves).

the ionomer. The following blend compositions in weight were prepared:

EVOH/PA: 80/20, 70/30, 50/50, 30/70.

EVOH/Ionomer: 90/10, 80/20, 70/30, 50/50, 30/70.

A selected number of blends of EVOH/PA and EVOH/ionomer were coextruded for tensile testing using conventional film coextrusion equipment. The extrusion of the blends was carried out using pelletised pre-extruded blends. LDPE top and bottom layers were coextruded (no tie layers were used) to sandwich the barrier (EVOH blend) layer. Before testing the multilayer system the PE layers were easily delaminated to release the inner EVOH blend film.

2.2. Thermal analysis

Differential scanning calorimetry (DSC) experiments were recorded using a Perkin–Elmer DSC7 calorimeter at a heating rate of 10°C/min on, typically, 6 mg of sample. The calibration of the DSC was carried out with a standard sample of indium. The same thermal history was given to all samples. This consisted of a first heating scan from room temperature to 225°C at 20°C/min, followed by an isothermal at 225°C for 1 min, and a subsequent cooling scan to room temperature at 100°C/min. Melting points and enthalpies were evaluated from the second heat run at 10°C/min. The glass transition temperature (T_g) was calculated from the second heat run of the sample using the so-called 'half C_p extrapolated' method. This method defines the T_g as the point on the curve where the 'specific heat' (C_p) change is half of the change in the completed transition. Crystallization points and enthalpies were determined from cooling scans from the melt at 10°C/min.

Dynamic mechanic analysis (DMA) experiments were carried out on compression molded polymer bars in a Perkin–Elmer DMA7e at a constant frequency of 1 Hz from −100 to 165°C at 5°C/min in the three point bending mode. Temperature calibration was carried out with water and indium.

2.3. WAXS

Wide angle X-ray scattering experiments were performed using a Siemens D5000D equipment. Radial scans of intensity versus scattering angle (2θ) were recorded at room temperature in the range 3–43° (step size: 0.03, time/step: 3 s) with identical settings of the instrument by using filtered CuK_α radiation ($\lambda = 1.54$ Å), an operating voltage of 40 kV, and a filament current of 30 mA.

The WAXS crystallinity of the isotropic samples was calculated using Eq. (1).

$$\%\chi\text{WAXS} = \frac{I_c}{(I_c + I_a)}100, \tag{1}$$

where I_c is the integrated area of the crystalline sharp reflections and I_a is the integrated area of the amorphous halo underneath the crystalline reflections. WAXS experimental data in the range 8–32° were processed with the curve-fitting routine in the Grams Research 2000 software package (Galactic Industries). Convolution of Lorentzian and Gaussian band shapes and linear baseline were used.

2.4. SEM

Scanning electron microscopy experiments were carried out in a Jeol JMS-6300. Samples were cryofractured and gold coated prior to SEM observations.

2.5. MH

A Vickers indenter attached to a Shimadzu MH tester was utilized for micro-indentation measurements at room temperature using a contact load of 0.49N and a contact time of 25 s. The MH values (in MPa) were calculated

Table 1
Melting (Mpt) and crystallization (Cpt) points, glass transition temperatures (T_g), overall WAXS crystallinity (χ_{WAXS}), WAXS crystallinity of the EVOH fraction ($^{EVOH}\chi_{WAXS}$), and melting ($\Delta H_{m\ EVOH}$) and crystallization ($\Delta H_{c\ EVOH}$) enthalpies of the EVOH fraction in the blends studied ((w) means weak peak, (s) means strong peak)

Blends	Mpt $_{EVOH}$ (°C)	Mpt $_{Ion.}$ (°C)	Cpt $_{EVOH}$ (°C)	Cpt $_{Ion.}$ (°C)	$T_{g\ EVOH}$ (°C)	$T_{g\ PA}$ (°C)	χ_{WAXs} (%)	$\Delta H_{m\ EVOH}$ (J/g)	$^{EVOH}\chi_{WAXS}$ (%)	$\Delta H_{c\ EVOH}$(J/g)
EVOH/PA blends										
EVOH	183.0	–	157.6 103.3(w)	–	59	–	35.2	75.8	35.2	76.2
80/20	183.7	–	158.6 104.6(w)	–	61	127	20.8	75.4	26.0	75.7
70/30	183.0	–	156.3 103.6(w)	–	60	125	18.8	76.2	26.8	77.4
30/70	182.7	–	157.3	–	62	125	6.6	66.0	22.1	88.0
PA	–	–	–	–	–	127	–	–	–	–
EVOH/ionomer blends										
EVOH	183.0	–	157.6 103.3(w)	–	59	–	35.2	75.8	35.2	76.2
90/10	185.4	96.0	159.0 105(w)	–	62	–	33.5	76.1	32.0	76.6
80/20	183.4	94.4	158.3 104.6(w)	66.3	61	–	31.8	74.8	35.1	77.2
70/30	184.4	95.0	158.3 104.3(w)	65.6	–	–	30.7	74.0	34.1	77.1
50/50	183.4	95.0	157.6 121.6(w)	73.3	–	–	28.6	76.0	34	74
30/70	182.4	95.0	159.3 121.3(s)	68.6	–	–	25.3	81.2	29.4	77.8
Ionomer	–	95.4 198(w)	–	64.3	–	–	19.6	–	–	–

from Eq. (2).

$$MH = \frac{2\sin 68^\circ P}{d^2}, \tag{2}$$

where P (in N) is the contact load y d (in mm) is the average of six measurements of diagonal length of the projected indentation area.

2.6. Tensile testing

Tensile testing to failure of the EVOH/PA melt-mixed blends was carried out at room temperature in an Instron 4400 Universal Tester. A fixed crosshead rate of 10 mm/min was utilized in all cases and the results were taken as the average of five tests. Dumb-bell shaped specimens were used according to the standard ASTM D638.

Tensile testing was also carried out at crosshead rates of 10 and 50 mm/min on extruded films of selected blends of EVOH/PA and EVOH/Ionomer.

3. Results and discussion

DSC cooling and heating experiments were conducted for all the samples to determine melting and crystallization points, the enthalpy associated with both processes and glass transition temperatures. Fig. 1 shows the endotherms and exotherms of neat EVOH and Ionomer, and the endotherm of PA. From Fig. 1, it can be easily detected in the heating scan the transitions associated with the T_g's of EVOH and PA at ca. 59 and 127°C, respectively, the melting peak of EVOH with maximum at 183°C and the two melting peaks of the ionomer at 95 and 198°C. The latter melting peak is very weak (6.1 J/g) and it is assigned to the crystalline polyamide fraction present in the ionomer. In the cooling runs, we can observe the crystallization peaks of EVOH at ca. 158°C and a weak exotherm at ca. 103°C, and the crystallization peak of the ionomer at ca. 64°C. The occurrence of a lower temperature crystallization shoulder at 103°C in neat EVOH points to molecular heterogeneity as suggested by the identification of material of low melting temperature by Fonseca et al. [19].

The melting and crystallization points, the associated enthalpies and the glass transition temperature for the blends are summarized in Table 1 and the corresponding heating endotherms shown in Fig. 2. From the observation of Fig. 2 and Table 1, it can be seen that, in general, the melting points are not greatly altered in the blends with regard to those of the parent polymers. By closer looking, it can be seen that in the blends with low contents of second component, in particular for the 90/10 EVOH/ionomer blend, a slight increase of up to ca. 2°C in the melting point of EVOH is observed. This behavior has been reported earlier in blends of EVOH and non-PA-containing ionomer by Samios et al. [5] and was attributed by the authors to synergy and increased order and interaction. From Table 1 it can also be seen that the blends show slight melting point

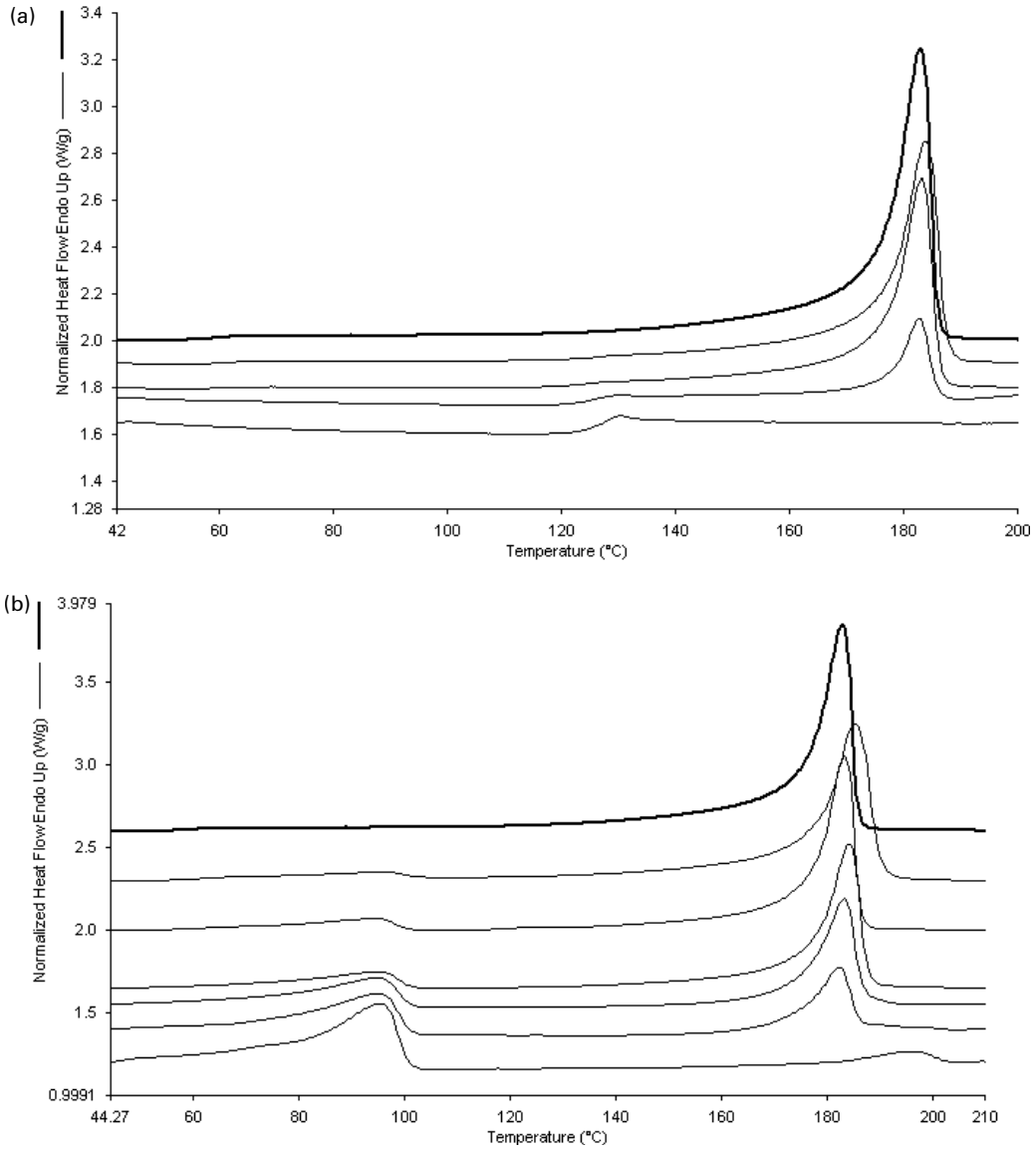

Fig. 2. (a) DSC melting endotherms of EVOH/PA blends, from top to bottom, 100/0, 80/20, 70/30, 30/70, 0/100. (b) DSC melting endotherms of EVOH/ionomer blends, from top to bottom, 100/0, 90/10, 8020, 70/30, 50/50, 30/70, 0/100.

depletion (by a maximum of ca. 3°C in EVOH/ionomer blends and of ca. 1°C in EVOH/PA blends) with increasing amorphous PA and inomer content in the blends.

In the crystallization runs (Fig. 3), the most relevant and surprising feature is the appearance of a third peak, in addition to the ones of EVOH and ionomer, with minimum at ca. 121°C in the 50/50 and 30/70 EVOH/ionomer blends (see Fig. 3b). The occurrence of this additional peak is reproducible, and it is attributed to the reduction in the crystallization temperature of an increasing part of the EVOH present in these EVOH/ionomer blends. Moreover, the crystallization temperature of the ionomer in these phase inversion blends is shifted toward higher temperature. The crystallization behavior of these particular blends suggests that an increasing part of the EVOH needs a higher undercooling before it can crystallize, possibly impaired by the presence of an increasing quantity of surrounding molten ionomer (diluent effect) or, more likely, induced by the crystalline polyamide present in the ionomer. The higher crystallization temperature seen for the ionomer in these blends indicates that possibly EVOH facilitates the crystallization of the ionomer by acting as a nucleating agent. A subsequent heating run of such crystallized blends showed no alterations in the melting points and enthalpies with regard to the values summarized in Table 1. Nevertheless, the latter observation may not necessarily rule out the presence of a different more imperfect EVOH crystallinity (originated from the lower undercooling needed to crystallize) in these ionomer rich blends. It is argued so because during the heating run the crystals may well undergo sufficient annealing to restore and consequently melt at the usual temperature (see later in the paper). The behavior observed

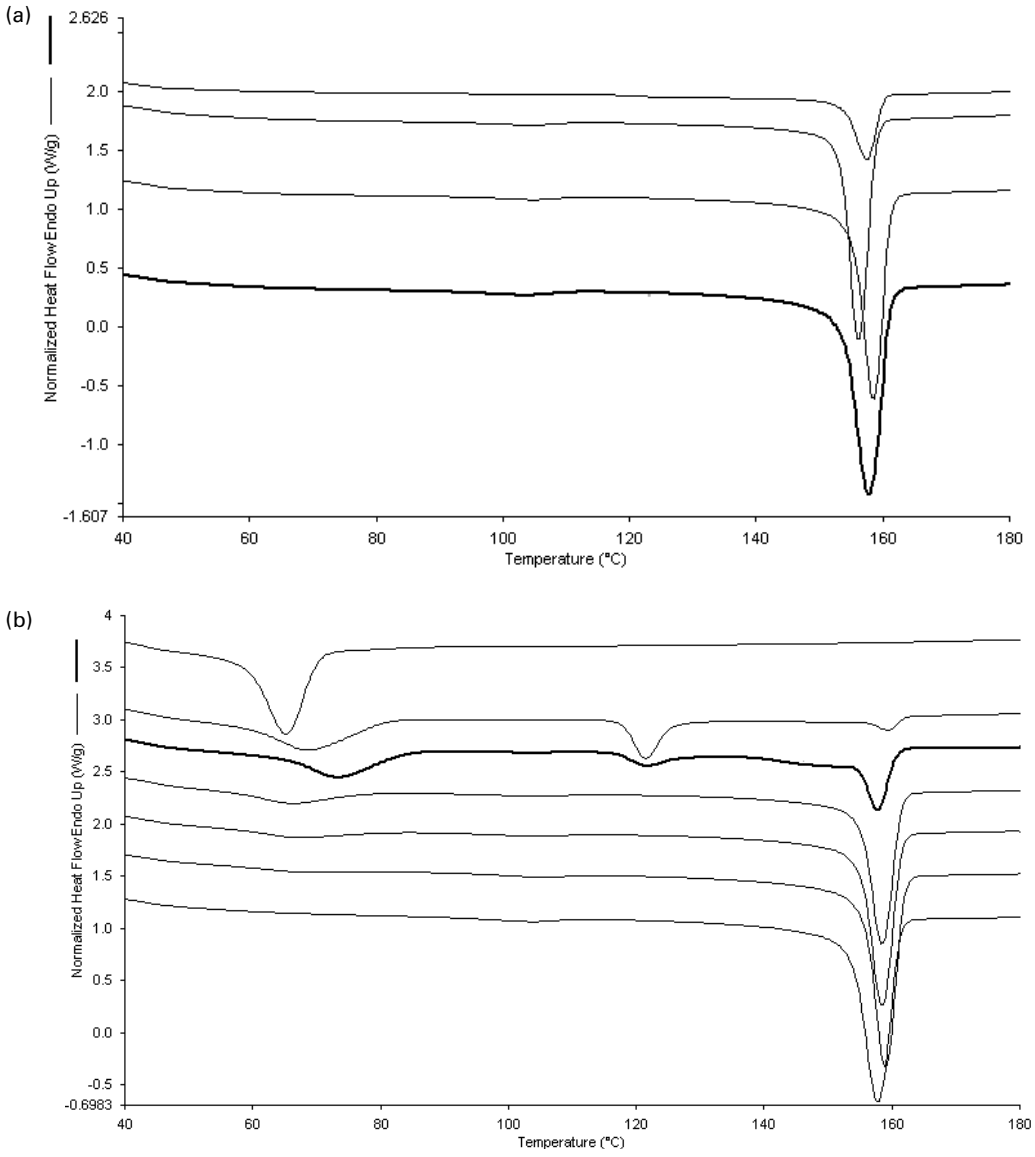

Fig. 3. (a) DSC crystallisation exotherms of EVOH/PA blends, from top to bottom, 0/100, 30/70, 70/30, 80/20, 100/0 (b) DSC crystallisation exotherms of EVOH/ionomer blends, from top to bottom, 0/100, 30/70, 50/50, 70/30, 80/20, 90/10, 100/0.

during crystallization in these phase inversion blends was not displayed by the ionomer studied by Samios et al. [5] and therefore must be attributed to a positive compatibilization effect of the crystalline PA present in the ionomer. A better compatibility between PA's and EVOH is always found in the PA rich blends [13].

Table 1 also shows the T_g of the blends as determined from the DSC heating scans. In the case of EVOH/PA blends we observe the presence of the T_g of the neat components. This indicates lack of thermodynamic miscibility between components in the blends, and was anticipated by the observation of no relevant changes in melting and crystallization points. Thermodynamic miscibility would have entailed the appearance of a composition dependent single T_g (in between the T_g's of the neat blend components) that usually follows either the Fox equation [20] or the Gordon–Taylor equation [21]. The compatibility of the EVOH/ionomer blends is difficult to asses by DSC because the T_g of EVOH is overlapped with the melting peak of the ionomer and because no second order transitions are unambiguously identified in the ionomer, even at subambient temperatures (see Fig. 4). From Fig. 4, a shoulder at the low temperature side of the ionomer melting peak, i.e. at about 75°C, can be seen. This feature may be attributed to low melting point crystals coming from structural heterogeneity. These crystals being responsible for the weak crystallization exotherm observed in Fig. 4 at about 40°C. Two glass transitions are often encountered in ionomers when measured by DSC or/and DMA [22]. These are associated to (i) the relaxation of the matrix, e.g. amorphous short chain segments containing polyethylene branches and non-ionized carboxylate groups, and (ii) to order-disorder transition in the ionic cluster. An

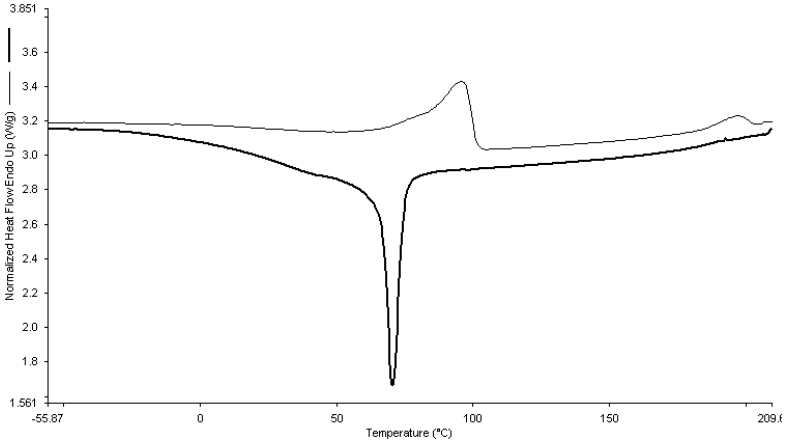

Fig. 4. Melting (top curve) and crystallisation (bottom curve) of polyamide-containing ionomer from −60 to 210°C.

ionic transition at ca. 44°C assigned to order-disorder transition in the ionic cluster has been reported in the DSC run of an inomer, Zn^{2+} containing no polyamide [5]. In this study, the above transitions are not observed, perhaps reflecting the structural and/or compositional differences exhibited by the ionomer used here. The T_g of EVOH in the 90/10 and 80/20 EVOH/ionomer blends could be measured (see Table 1) and showed a value slightly higher than that for neat EVOH. In the EVOH/ionomer blends with higher contents of ionomer the T_g of EVOH was not detected.

In spite of the fact that miscibility was not observed, the two T_g's of the EVOH/PA blends appeared slightly shifted towards each other with regard to those of the neat components. This is particularly the case of the 70/30 blend. These observations may suggest some degree of interaction between blend components, presumably at the domains interface. Fig. 5a shows the loss modulus curves for EVOH, PA and the 80/20 EVOH/PA blend. This figure shows that the main relaxation peaks of the neat components, i.e. at 67°C for EVOH (α-peak) and 118°C for neat PA, are almost unchanged in the 80/20 blend, i.e. at 65 and 117°C in the blend, in excellent agreement with the DSC results. In view of the fact that the determination of T_g by DSC could not be undertaken successfully in the EVOH/ionomer blends, complementary DMA experiments were also carried out in the EVOH/ionomer blends to assess blend components compatibility (see Fig. 5b). From Fig. 5b a broad relaxation is observed for the ionomer centered at around 20°C. The 80/20 EVOH/ionomer blend clearly show the main relaxation of EVOH (α-peak) at around 65°C. A lower temperature relaxation peak is also seen in this blend which could arise from the superposition of the low temperature peak of EVOH (β-peak) and the ionomer broad relaxation. The rest of EVOH/ionomer blends does not show the α-peak of EVOH but a lower temperature peak. This could be interpreted as a shift of the T_g of EVOH toward lower temperature and therefore a better compatibilization between blend components in the ionomer rich blends. At this point, it should be remarked that although it is well accepted and extended the use of the DMA technique to support discussions about polymer miscibility in blends, and consequently this technique has been used in a number of cases to report about the compatibility of EVOH and other polymers, it is found that the shape of the DMA curves of EVOH is strongly dependent on factors like (i) specimen obtaining conditions (slow cooling as opposed to quenching), (ii) specimen annealing conditions in quenched materials and, evidently, on (iii) relative humidity or sorbed moisture. As an example, Fig. 6 shows the DMA tanδ of a severely crash cooled sample after drying at 110°C for 1 h, after annealing at 150°C for 30 min and after annealing a 170°C for 30 min. In this figure, it can be observed that originally tree relaxations are observed which change position and intensity after severe annealing. Annealing of EVOH does result in structural changes like phase transformation from orthorhombic to monoclinic, increase in crystallinity (see below) and perhaps stiffening in the amorphous phase. The stiffening is suggested by the shift of the α-peak (associated with the polymer T_g) toward higher temperature with intensifying the annealing conditions. On the other hand, the lower temperature relaxation (β-peak or sub-T_g) decreases intensity and also shifts toward higher temperature. The assignment of this peak is uncertain. The higher temperature relaxation (α_c-peak) results, for analogy with polyethylene and other highly crystallized polymers, from low mobility in the crystalline phase [13]. From Fig. 6 this α_c-peak shifts toward higher temperature for severely annealed samples showing monoclinic crystallinity (see below). Slow cooled samples also have crystals with the thermodynamically more stable monoclinic symmetry and the α_c-peak also appears at a higher temperature. The cited effects do have a marked impact on the polymer morphology and in the shape of the DMA curves, and therefore a careful analysis of the results in terms of polymer compatibility must be carried out for this polymer.

Crystallinity and crystalline morphology for the blends

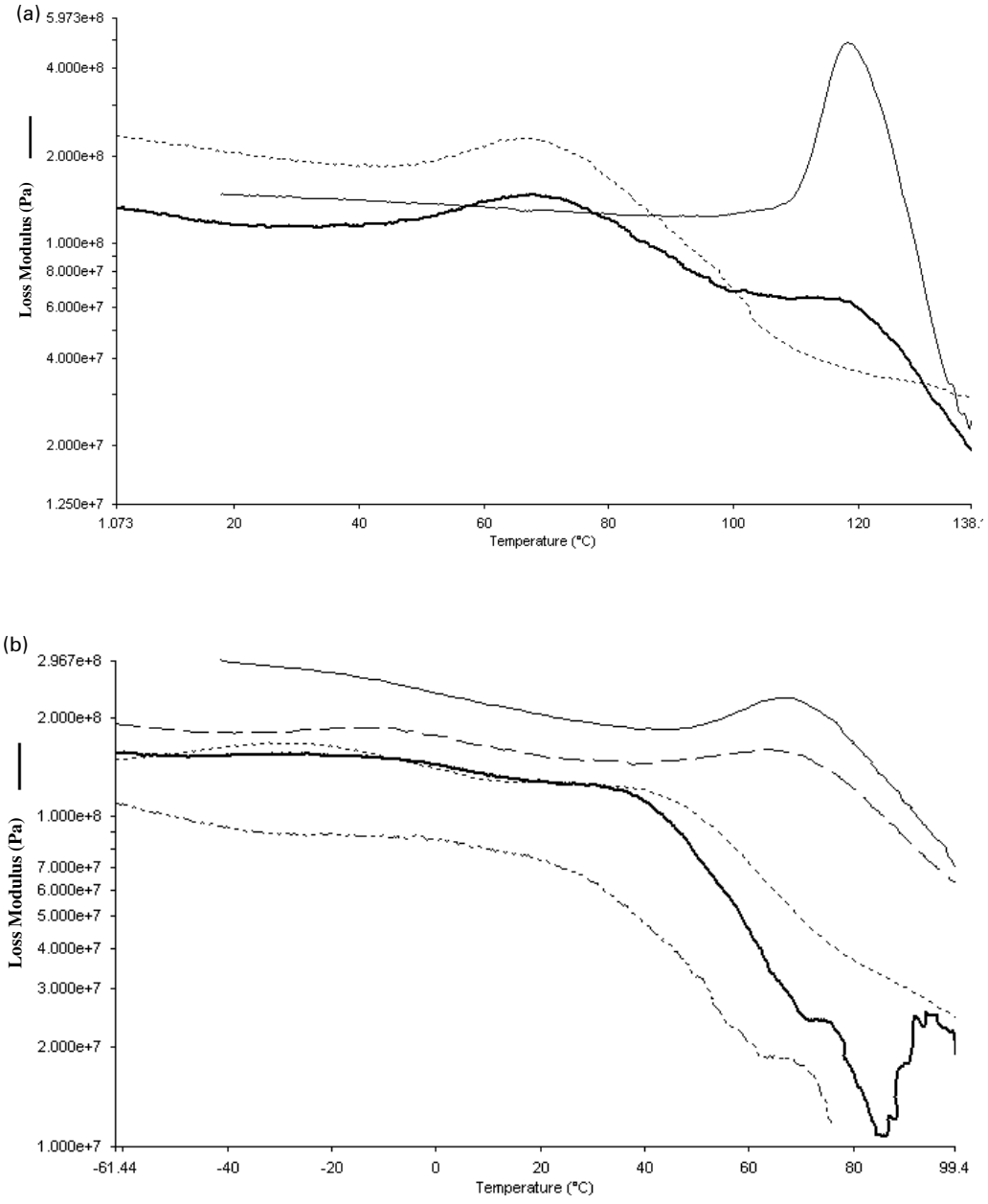

Fig. 5. DMA loss modulus curves of (a) EVOH (continuous curve), 80/20 EVOH/PA blend (thicker curve) and amorphous polyamide (dotted curve); and of (b) EVOH/ionomer blends, from top to bottom, EVOH, 80/20 (dashed curve), 70/30 (dotted curve), 50/50 and ionomer.

was determined by means of WAXS experiments (see Fig. 7 and Table 1). From Fig. 7, the crystalline morphology of EVOH appears to be orthorhombic throughout blend composition. Two major reflections are seen for EVOH at angles 20.2 and 21.9° characteristics of a pseudohexagonal or orthorhombic lattice [23], which decrease presence in the phase inversion blends. It is known that, thermodynamically, the most stable lattice for this EVOH copolymer is a monoclinic lattice similar to that exhibited by the parent polyvinyl alcohol polymer. A monoclinic crystalline symmetry was obtained by slow cooling or by severe annealing of a quenched EVOH sample (see Fig. 8). As the blends reported here were obtained by quenching from the melt the orthorhombic morphology is observed in all cases. In the blends the diffraction patterns of the EVOH (highest crystallinity constituent of the blends) decrease with increasing blending component content and therefore the overall crystallinity of the blends is reduced (see Table 1). This reduction is seen much higher for EVOH/PA blends because the PA is amorphous. The crystallinity of the EVOH normalized for its content in the blends appears to decrease slightly by WAXS, and slightly more in the blends with PA. It should be borne in mind though the curve-fitting becomes more complex in the phase inversion blends due to overlapping of features and weakening of the crystalline patterns. Enthalpies of fusion and crystallization for the

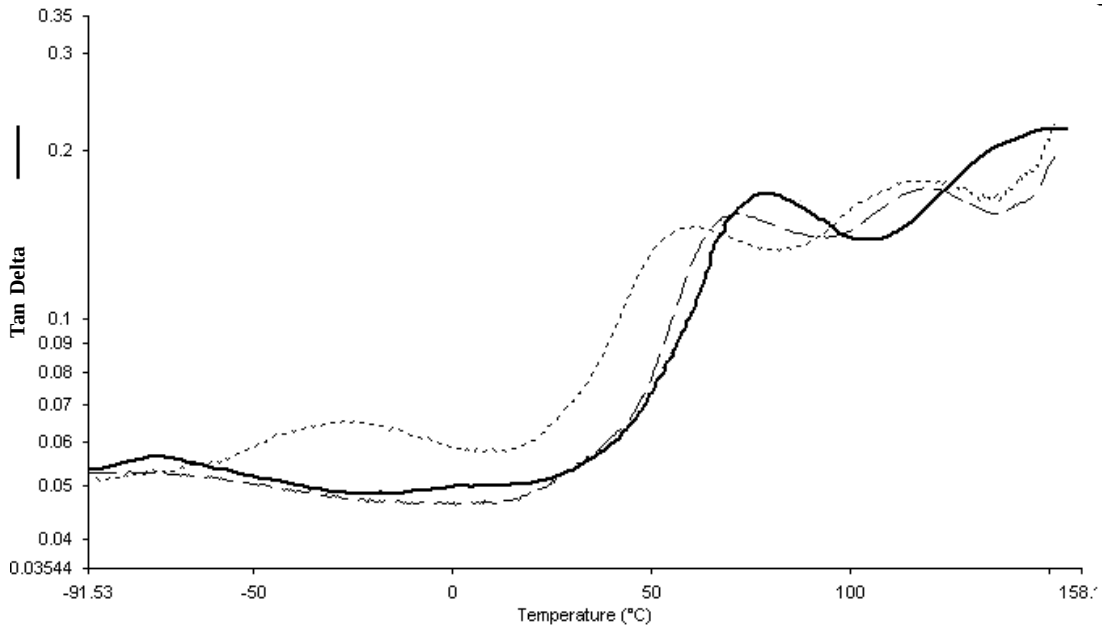

Fig. 6. DMA loss modulus curves of dry fast-cooled EVOH (dotted curve), after annealing at 150°C for 30 min (dashed curve) and after annealing at 170°C for 30 min (thicker curve).

EVOH fraction in the blends are also given in Table 1. In the enthalpy of crystallization, it was included the exothermic shoulder seen for EVOH at around 103°C and, of course, the peak at around 121°C seen in the phase inversion EVOH/ionomer blends. In general, melting and crystallization enthalpies are largely unaltered throughout blend composition. Nevertheless, in two cases some variations are seen. Thus, the heat of fusion of the 30/70 EVOH/PA blend is seen slightly lower and the heat of crystallization slightly higher. The reason for the lower heat of fusion for the latter blend could arise from a genuine crystallinity drop, albeit may also arise from experimental error because the fraction of EVOH in this blend is already very low. The higher heat of crystallization in this blend is definitely ascribed to the impact that the T_g of the PA present in the blend has over the integration of the exotherm. Changes in the baseline of the endotherms and exotherms between different samples due to the presence/absence of second order transitions have also some impact in the measurements. To avoid this influence over the heat of fusion, the integration of the endotherms was carried out from 130°C in the blends. The blend 30/70 EVOH/ionomer does show somewhat higher heat of fusion. This effect is attributed to the inclusion in the integration of part of the melting feature of the PA present in the ionomer and showing underneath the EVOH peak at the high temperature side. Summarizing, the crystallinity of the EVOH fraction present in the blends is either unaffected as suggested from the DSC results or slightly lower as suggested by WAXS.

In this respect, it was also encountered that the determination of the absolute crystalline fraction present in neat EVOH is far from being a straightforward matter. Thus, while WAXS measures a crystallinity value for quenched EVOH of 35% and for slow cooled samples of 55%, in good agreement with data reported in the literature [23], the DSC melting enthalpy always yields, irrespective of obtaining procedure, a crystallinity value of ca. 70% (using a reference value for the enthalpy of fusion of a perfect EVOH crystal, ΔH_f^{EVOH}, of 106 J/g [24]). A lack of consistency between crystallinity data as obtained from the use of different techniques is often common in polymers and has its origin in the methodologies applied, the assumptions made and/or in the inherent instrumental limitations [24–28]. Some authors [5,24] utilize the above value of 106 J/g as the enthalpy of fusion of a perfect EVOH crystal to estimate the crystallinity of EVOH samples. This number is calculated from the simple relation $\Delta H_f^{EVOH} = \alpha \Delta H_f^{PVOH}$, where α is the mole fraction of polyvinyl alcohol (PVOH) in the copolymer and ΔH_f^{PVOH} is the heat of fusion of a perfect monoclinic crystal of PVOH at 156.2 J/g [29]. In our opinion, this methodology does not appear to be justified because if a simple additive rule was going to be used the ΔH_f^{PE} of orthorhombic polyethylene should also be considered in the calculations. Moreover, it is worthy to remark that no monoclinic symmetry crystals but rather orthorhombic or similar are obtained in fast cooled and crash-cooled samples and in the blends. Therefore, an alternative approach to approximate a better value for ΔH_f^{EVOH} could derive from the use of the WAXS crystallinity as input [13]. By doing that we come up with a value for ΔH_f^{EVOH} of 216.6 J/g in the case of crash cooled orthorhombic EVOH. This value is intermediate between the ΔH_f^{PE} of orthorhombic polyethylene at 290 J/g [30] and the ΔH_f^{PVOH} of PVOH at 156.2 J/g. On the other hand, a value for ΔH_f^{EVOH} of 138 J/g

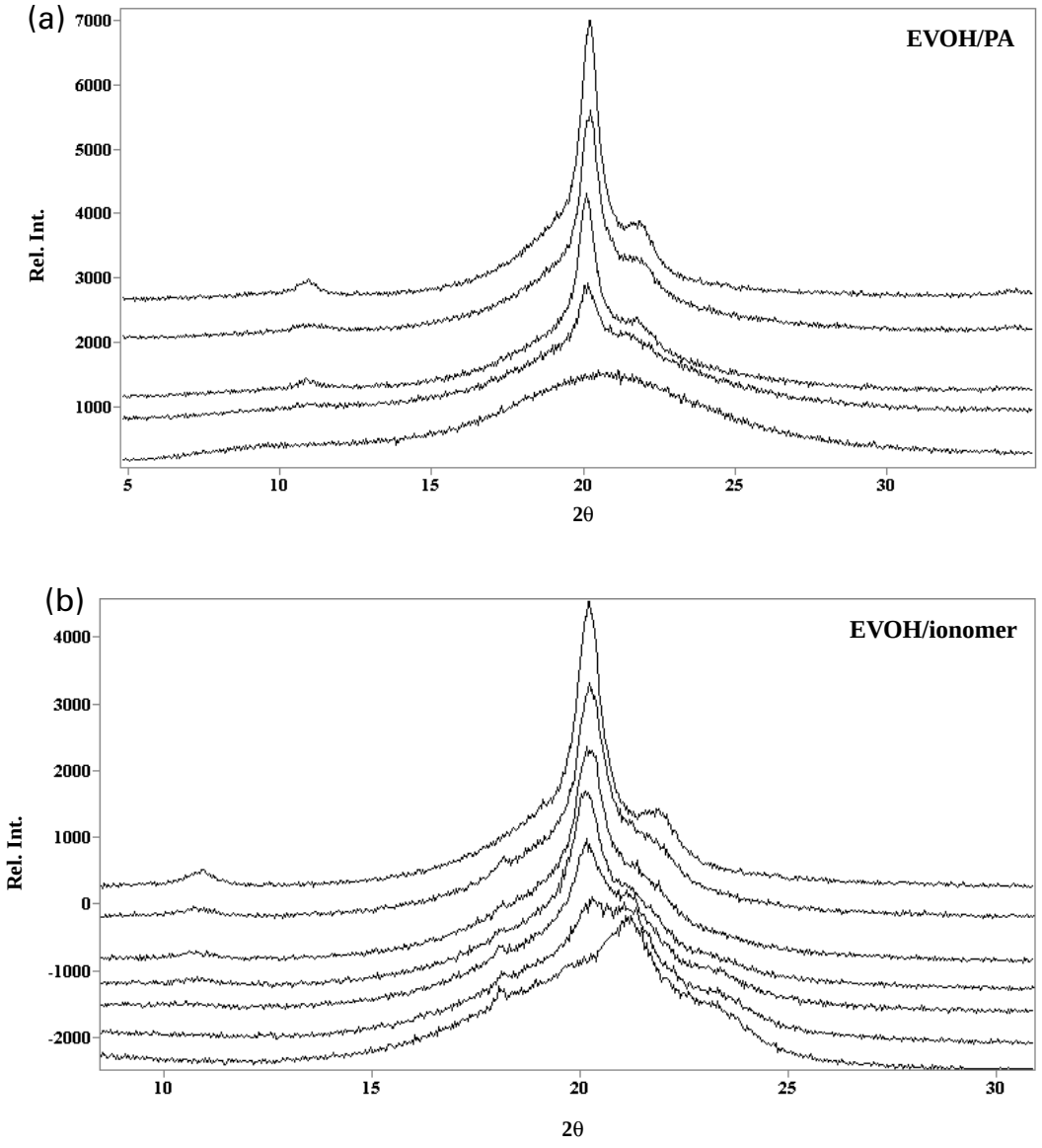

Fig. 7. WAXS diffraction patterns of (a) EVOH/PA blends with compositions, from top to bottom, 100/0, 80/20, 70/30, 30/70, 0/100; and of (b) EVOH/ionomer blends with compositions, from top to bottom, 100/0, 90/10, 80/20, 70/30, 50/50, 30/70, 0/100.

is obtained for a slow cooled monoclinic EVOH sample, indeed closer to ΔH_f^{PVOH}. Cerrada et al. [23] studied the WAXS crystallinity and DSC melting enthalpies of EVOH samples obtained at different cooling rates from the melt. While clear differences were measured by WAXS, no significant changes were measured by DSC in the samples. Their results are reproduced in the present study with great accuracy. The discrepancy in crystallinity data between the two techniques could be attributed to the EVOH samples developing crystallinity during the DSC run and reaching melting, irrespective of cooling rate, under the monoclinic form. Crystallinity development and polymorph change via solid–solid phase transformation during the DSC heating run occurs for instance in aliphatic polyketones [26,31]. If this was the case, the value to be used, as best estimate, for the ΔH_f^{EVOH} should be 138 J/g, which then yields a DSC crystallinity for EVOH of ca. 55%.

Scanning electron microscopy observations were carried out on cryofractured specimens of some blends (see Fig. 9). From this figure it can be seen that a fine phase separation occurs throughout composition in the blends at a microscopic level. This is revealed by the observation of dispersed segregated isometric particles in the blends. Particle size is in general less than two microns. Moreover, the observation of extensive debonding at the particle interface resulting in hollows suggest poor adhesion at the interface between blend components. The latter effect appears to be diminished in the EVOH/ionomer blends with high contents of ionomer. The above observations are therefore in agreement

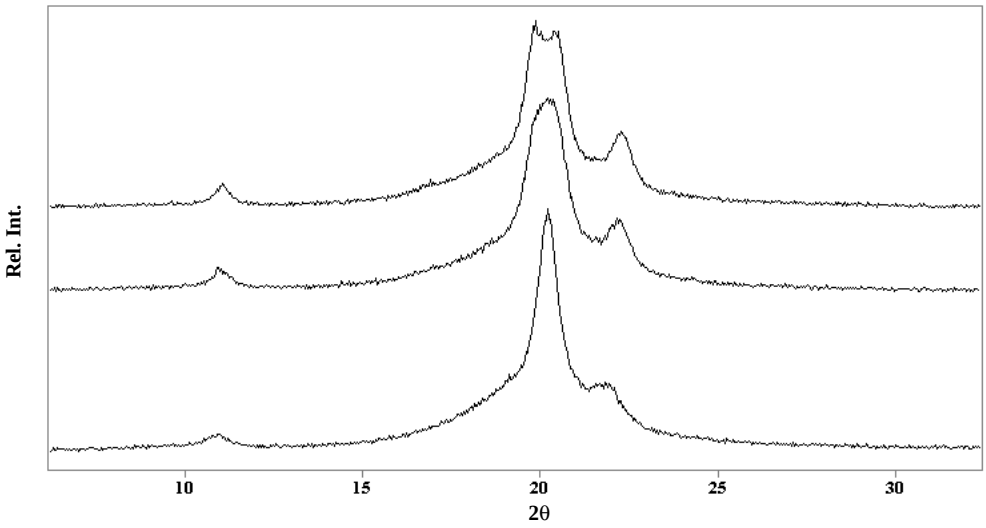

Fig. 8. WAXS diffraction patterns of, from top to bottom, slow cooled EVOH, crash cooled EVOH after annealing at 170°C and crash cooled EVOH.

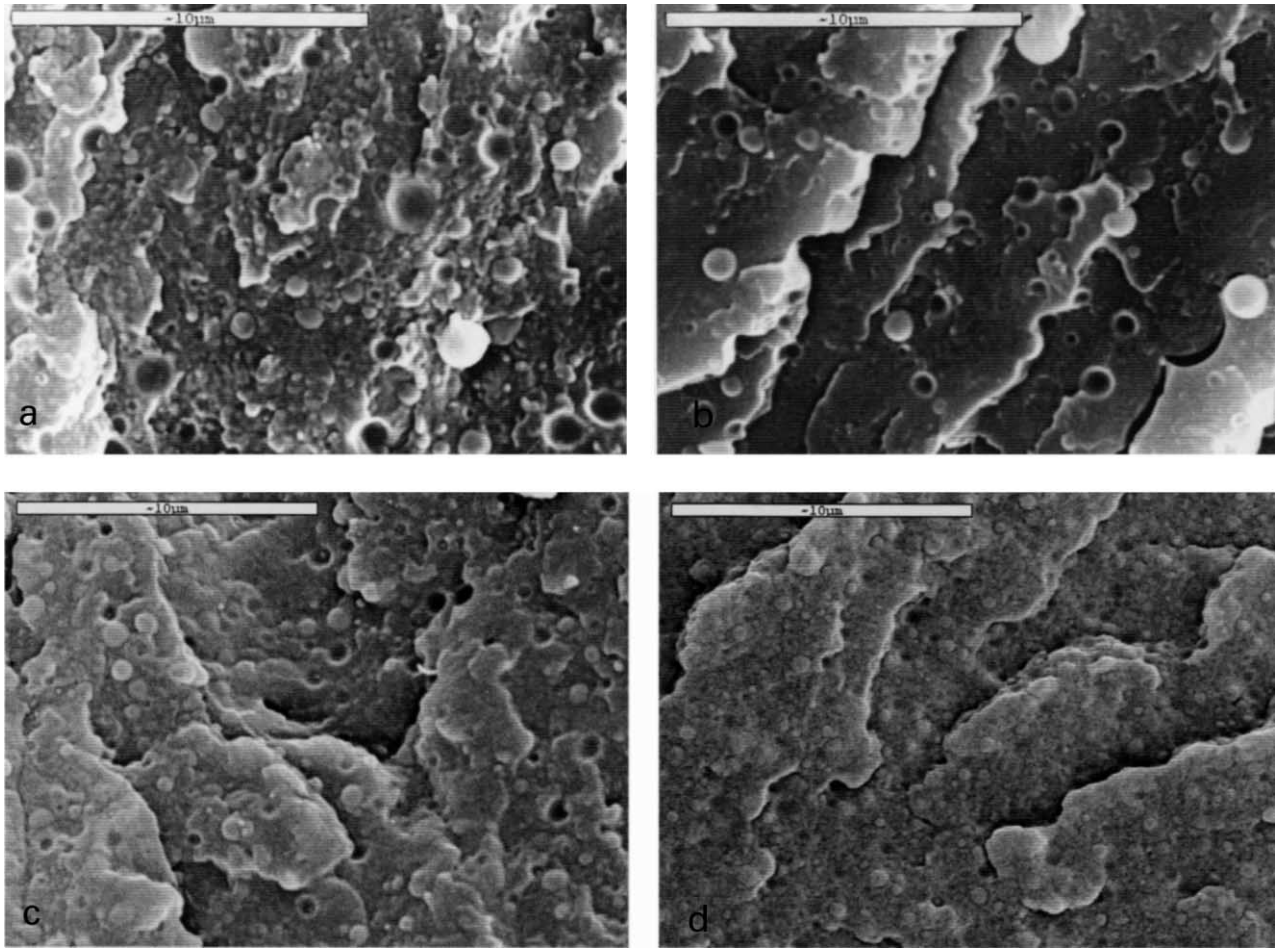

Fig. 9. SEM micrographs of (a) EVOH/PA 80/20 blend, (b) EVOH/PA 30/70 blend, (c) EVOH/ionomer 80/20 blend, (d) EVOH/ionomer 30/70 blend.

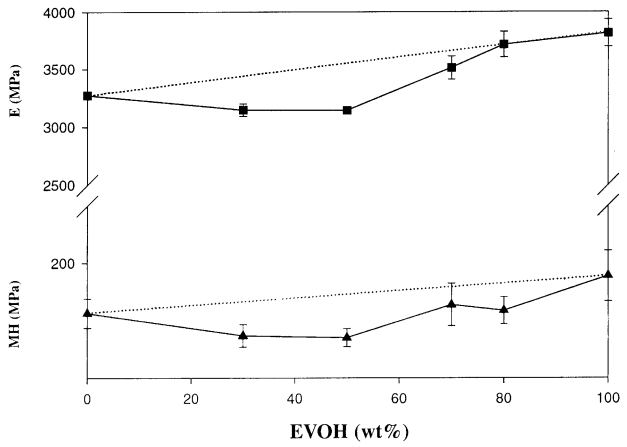

Fig. 10. Plot of MH and Tensile modulus (E) versus EVOH content in EVOH/PA blends.

with the previous data from which phase separation was anticipated.

The mechanical performance of the EVOH/PA blends was studied by MH and tensile experiments at room temperature in dry specimens. Fig. 10 shows the MH Vickers and tensile modulus as a function of EVOH content. This figure reveals that both magnitudes drop in the blends with regard to neat EVOH. The tensile modulus of the PA is slightly lower than that of EVOH at room temperature. From Fig. 10, a non-linear dependence with composition with a negative deviation from the simple additive rule is observed. The negative deviation is larger in compositions close to the phase inversion and lower for the blends with contents of PA below 30%. Strain to failure and toughness are shown in Fig. 11a and b, respectively, for all the EVOH/PA blends. From this figure we can observe that the PA and PA blends exhibit a clear brittle behavior at room temperature. Ultimate strain and toughness are in all the blends lower than those of neat EVOH. Furthermore, a negative deviation in the mechanical properties throughout composition suggests again non-miscible systems with very poor stress transfer at the domains interface in agreement with the SEM observations.

Film extrusion of both types of blends was trial successfully in our laboratories and the film quality and transparency was deemed good in general and excellent in the case of EVOH/ionomer blends. We must realize that in order to keep up the barrier performance of these blends a high content of EVOH must be present, hence our interest is in the performance of high EVOH content blends. Table 2 shows some of the mechanical data gathered in die-stamped dumb-bells in the machine direction for these films. Blends of EVOH and amorphous PA show a very brittle behavior, i.e. low extensibility and toughness, at the two cross-head rates used in good agreement with data shown above for compression molded specimens. Albeit, we hypothesized about the potential of some interaction between EVOH/PA blend components on the bases of slight variations in T_g, melting and crystallization points throughout composition, this possible interaction does not appear to be good enough to ensure good stress transfer between components. On the other hand, EVOH/ionomer blends show lower modulus than EVOH/PA blends but much higher extensibility (strain at break) and toughness. Ultimate strain and toughness increase in the 70/30 EVOH/ionomer blend and become higher than those of neat EVOH when the strain rate increases from 10 to 50 mm/min. By increasing deformation rate the heat developed during deformation does not dissipate as well as it would do at a lower strain rate and thus may enhance the blend temperature. This in turn may promote the flexibilizing role of the ionomer in the blends. This observation indicates that blending EVOH with ionomer may have processing advantages during, for instance, solid phase forming. Samios et al. [5] found a similar ionomer induced flexibilizing effect in tensile experiments at 100 mm/min. The presence of some crystalline nylon in the ionomer may seek a better interaction between ionomer and EVOH, high temperature processing improvements, and/or perhaps some higher temperature consistency as the nylon melts at 198°C. Blending EVOH with an amorphous polyamide or an ionomer appears to be justified. Nevertheless, the role of these blends is engineered to be fully displayed in the presence of moisture and probably in the high temperature performance of the material, i.e. during

Table 2
Tensile modulus (E), ultimate strain (ϵ_b) and toughness measured in extruded films of some of the blends at strain rates of 10 and 50 mm/min

Blends	10 mm/min			50 mm/min		
	E (Mpa)	ϵ_b (%)	Tough. (J/cm^3)	E (MPa)	ϵ_b (%)	Tough. (J/cm^3)
EVOH/PA extruded films						
100/0	2754 ± 66	43 ± 10	29	3137 + 183	65 ± 20	52
80/20	2706 ± 93	9 ± 2	6	2929 + 110	8 ± 1	5
0/100	2549 ± 153	5 ± 1	4	2731 + 152	5 ± 0.5	3
EVOH/ionomer extruded films						
100/0	2754 ± 66	43 ± 10	29	3137 + 183	65 ± 20	52
80/20	2340 ± 117	37 ± 10	23	2671 ± 115	50 ± 14	37
70/30	1807 ± 34	47 ± 0.5	18	2208 ± 43	155 ± 26	84
0/100	289 ± 24	164 ± 4	26	–	–	–

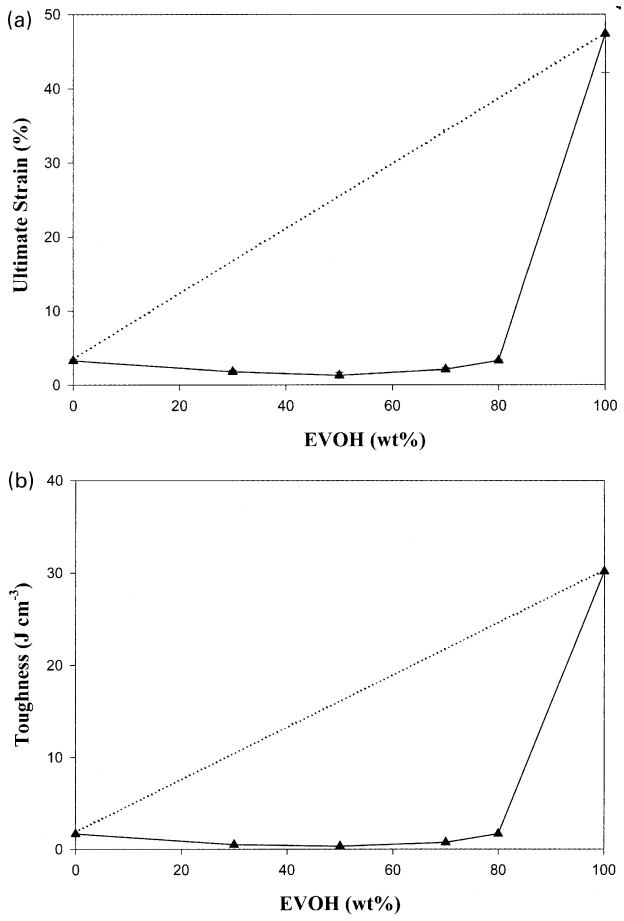

Fig. 11. Plot of (a) ultimate strain and (b) toughness versus EVOH content in EVOH/PA blends.

solid phase thermoforming. In support of the latter is the observation of the low hygrospicity exhibited by the ionomer and the higher material strength exhibited by blends of EVOH with amorphous PA in the presence of moisture [32]. Moreover, the amorphous PA shows improved barrier properties at high relative humidity conditions.

4. Conclusions

A number of binary blends of high barrier EVOH with amorphous PA and PA containing EVOH have been carried out by thermal analysis, dynamic-mechanical analysis, WAXS, SEM, MH and tensile testing. In EVOH/PA blends a lack of good compatibility was found. Thus, although some variations in melting point and slight T_g shifts were observed in the EVOH/PA blends, extensive debonding at the domains interface as suggested by SEM and negative deviation in the mechanical properties pointed to a lack of good interaction between blend components. The compatibility exhibited by the blends of EVOH and amorphous PA is found to be lower than that described in the literature for EVOH/PA6 blends. For the latter blends, the variation across composition in melting point, crystallinity and T_g were reported to be greater [6,8,11]. The lack of good interaction may arise from differences in geometric hindrance and stiffness of the amorphous PA when compared with PA6 [14]. Some better blend components interaction and synergy was exhibited by EVOH/ionomer blends. Ionomer rich blends did reduce the crystallization temperature of part of EVOH and the DMA traces suggested best interaction between blend components. Perhaps the presence of crystalline nylon in the ionomer could enhance the interaction with EVOH; Samios et al. [5] proved that some genuine compatibility exist between a similar ionomer and EVOH provided by hydrogen bonding or ionic interactions. Blend film coextrusion was carried out successfully and the barrier film showed excellent transparency and lack of gels. EVOH/ionomer blends showed increased flexibility and toughness. Thermoformability characteristics of extruded films and barrier properties as a function of relative humidity are now under study to assess whether these blends can become a technological advantage in film packaging. The strong degree of self-association predicted and exhibited by high barrier EVOH (with 32 mol% of ethylene) copolymer is again highlighted here.

Acknowledgements

AIMPLAS (Technology Park, Valencia, Spain) is thanked for experimental support. This work was supported by Ministerio de Educaciòn y Cultura I + D, Mat. Program IFD97-0813-CO3.

References

[1] Foster RH. Polym News 1986;11:264.
[2] Lagaron JM, Powell AK, Bonner JG. Polym Testing 2001;20(5):569.
[3] Chou R, Lee IH. J Plastic Film Sheeting 1997;13:74.
[4] Coleman MM, Yang X, Zhang H, Painter PC. J Macromol Sci-Phys 1993;B32(3):295.
[5] Samios CK, Kalfoglou NK. Polymer 1998;39:3863.
[6] Petris S, Laurienzo P, Malinconico M, Pracella M, Zendron M. J Appl Polym Sci 1998;68:637.
[7] Lohfink GW, Kamal MR. Polym Ing Sci 1993;33:1404.
[8] Lee SY, Kim SC. J Appl Polym Sci 1998;67:2001.
[9] Uno M, Norton LJ, Kramer EJ, Oda H. J Mater Sci 1998;33:853.
[10] Russo P, Acierno D, Di Maio L, Demma G. Eur Polym J 1999;35:1261.
[11] Ahn TO, Kim CK, Kim BK, Jeong HM, Hum JD. Polym Engng Sci 1990;30:341.
[12] Akiba I, Akiyama S. Polym J 1994;26:873.
[13] Nir Y, Narkis M, Siegmann A. Polym Engng Sci 1998;38:1890.
[14] Liu Y, Donovan JA. Polymer 1995;36:4797.
[15] Hernandez RJ, Giacin JR, Grulke EA. J Membr Sci 1992;65:187.
[16] Aucejo S, Marco C, Gavara R. J Appl Polym Sci 1999;74:1201.
[17] Zhang Z, Britt IJ, Tung MA. J Polym Sci: Part B: Polym Phys 1999;37:691.
[18] Fetell AI. 1997 TAPPI Polym. Laminations and Coatings Conference, August 24–28 1997.

[19] Fonseca C, Pereña JM, Benavente R, Cerrada ML, Bello A, Perez E. Polymer 1995;36:1887.
[20] Fox TG. Bull Am Phys Soc 1956;1:123.
[21] Gordon M, Taylor JS. J Appl Chem 1956;2:495.
[22] Eisenberg A, Kim J-S. Introduction to ionomers. New York: Wiley, 1998.
[23] Cerrada ML, Perez E, Pereña JM, Benavente R. Macromolecules 1998;31:2559.
[24] Faisant JB, Ait-Kadi A, Bousmina M, Deschenes L. Polymer 1998;39:533.
[25] Balta Calleja FJ, Vonk CG. X-ray scattering of synthetic polymers. Amsterdam: Elsevier, 1989.
[26] Lagaron JM, Vickers ME, Powell AK, Davidson NS. Polymer 2000;41:3011.
[27] Lagaron JM, Dixon NM, Reed W, Pastor JM, Kip BJ. Polymer 1999;40:2569.
[28] Lagaron JM, Lopez-Quintana S, Rodriguez JC, Pastor JM. Polymer 2000;41:2999.
[29] Hwang KS, Lin CA, Lin CH. J Appl Polym Sci 1994;52:181.
[30] Bershtain VA, Egorov VM. Differential scanning calorimetry of polymers. Chichester, UK: Ellis Horwood, 1994.
[31] Lagaron JM, Powell AK, Davidson NS. Macromolecules 2000;33:1030.
[32] Lagaron JM, Gimenez E, Saura J. To be published.